Examples

Figure 4 shows two measurements that are strongly affected by noise from a nearby power line (record to the left). A stack of $N = 3$ shows a considerable improvement of the S/N ratio (center record). The current is shown to the right of the figure. The gradual improvement of the signal during successive stacks is shown in Figure 5. The impulse widths of the normal and reversed current (bottom) are asymmetric. At a stack of $N = 4$ (top), the noise/signal ratio is 12.7 percent. Successive increases of stacks to $N = 8$ and 12 reduce this ratio to 5.5 and 4.25 percent, respectively. This improvement can also be recognized on the voltage plots.

Finally, an example of an impulse deformation is shown in Figure 6. The voltage records show from top to bottom a 3, 6, and 9 stacked sequence. The stack with $N = 9$ clearly shows an impulse deformation that is characteristic for an IP effect. This measurement was conducted over karst aquifers with a nearby sink hole development. The IP effect is explained by water and partially clay-filled fissures, representing good conductors, which are separated by nonconducting compact limestone.

Summary

There are many applications of the electrical resistivity method for which analog systems seem to be inadequate. A computer-controlled digital measuring system has many advantages over conventional systems that are presently being used. Many geohydrological problems can be solved with accurate, reliable, and flexible resistivity systems. The correlation of permeabilities with the formation factor, groundwater pollution, karst hydrogeology, and the fresh water-salt water interface have been investigated with the resistivity method with varying success. Progress in these areas is only possible with a reliable, high-resolution measuring technique. One of the most challenging tasks is the application of the resistivity method for the location of hydrocarbon deposits. Here a major problem is the need to increase the depth of exploration. This cannot be solved with an increase of the electrode current alone, which would unnecessarily increase continuing operation costs. Electrical conductivity anomalies are associated with hydrocarbon deposits that affect the resistivity and induced polarization in very specific ways, which require a flexible, high resolution instrumentation.

A Portable Tensor Magnetotelluric   EM4.3
Receiver Design and Field Test

V. F. Labson, F. C. Frischknecht, U.S.G.S.; and A. Becker, Univ. of California, Berkeley

A prototype of a portable natural electromagnetic field receiver capable of in-field processing of audio-frequency tipper and magnetotelluric impedance measurements was developed. We tested it over a massive sulfide deposit in Maine using the remote reference technique. Two tipper profiles and several impedance soundings were acquired over the approximate frequency range 2.5-100 Hz. The data are of high quality and the tipper profiles clearly show the conductive massive sulfides as well as a conductive pyrrhotitic hornfels. The tipper data compare favorably with slingram and very-low frequency (VLF) data in the same area.
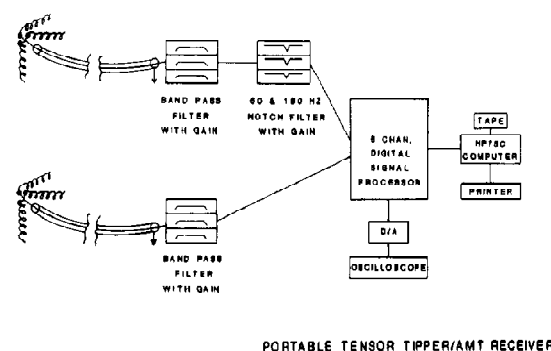

PORTABLE TENSOR TIPPER/AMT RECEIVER

Fig. 1. Block diagram of portable system.

Introduction

Subsurface mapping of electrical conductivity structure can be accomplished using the Earth's natural audio-frequency electromagnetic fields as an energy source. Most natural EM field systems are bulky and are intended for use in trucks. We developed and tested a prototype of a portable system capable of in-field processing of tipper and MT impedance measurements using the remote reference technique.

The portable receiver has two distinct advantages over truck mounted systems. The first advantage is portability; the two profiles surveyed in Maine were inaccessible by road and could have been acquired only with a portable system. The second advantage is the absence of an ac power source, which is frequently the dominant artificial noise source in natural field receivers. The portable receiver is completely dc powered. Because of the low noise level, good results were obtained with shorter recording times than with previous truck mounted systems.

Receiver

The receiver has a bandwidth of 10^{-3}-250 Hz but this test was limited to the frequency range of 2.5-100 Hz. The receiver (Figure 1) includes an analog section with induction coil magnetometers, preamplifiers, powerline notch filters, and band-pass filters. To make impedance measurements, electric field dipoles and amplifiers are added. The digital section is composed of the University of California–Lawrence Berkeley Laboratory EM-60 digital signal processor (Morrison et al., 1978) and a Hewlett-Packard 75C computer with printer and digital cassette tape recorder.[1]

The receiver acquires 6 channels of data simultaneously with 12-bit accuracy. The tipper is a measure of the vertical magnetic field relative to the horizontal magnetic field; Jupp and Vozoff (1976) gave a complete discussion of tipper quantities. Tipper results are computed as magnitude, dip direction, and phase, and the impedance is computed as principal directions, and apparent resistivity and phase in the principal directions. The tipper and impedance are both estimated from natural field power spectra using the remote reference technique (Gamble et al., 1979).

Tipper measurements are acquired at two stations simultaneously. At each station there are three magnetic field sensors oriented in x, y, and z directions. The horizontal fields measured at one station provide the remote reference for the other. The impedance tensor is measured by substi-
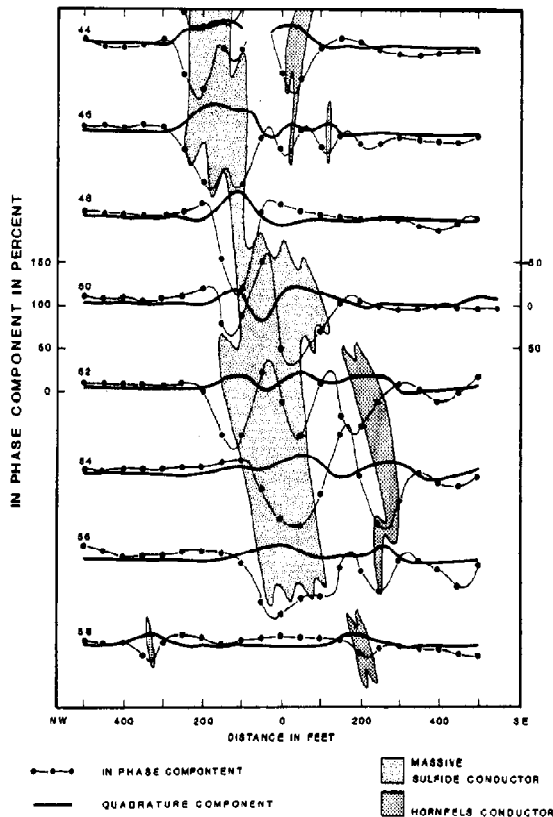
FIG. 2. Slingram profiles and outline of southwestern part of conductors: coil spacing = 100 ft, frequency = 600 Hz.

battery. The oscilloscope is powered by a similar battery. The sensors and computer are powered by small internal batteries. All of the batteries are sufficient for an entire day of field operation and are recharged each night.

Field site

The Burnt Nubble Cu-Ni-Co deposit occurs along the southeastern border of the Moxie pluton in Squaretown township in northwestern Maine (Espenshade, 1972). The pluton intrudes sedimentary rocks of probable Devonian age. In the vicinity of the deposit the pluton is composed primarily of gabbro and norite. Rocks on the southeastern side of the pluton are limey siltstones and slates, non-limey siltstones and slates, and pyrrhotitic slate and siltstone. Within about 1 000 ft of the contact, these rocks have been thermally metamorphosed to hornfels. The mineralized zones occur within the pluton. Results from 10 drill holes indicate that the deposit is heterogeneous and consists of stringers of massive sulfides, ranging from inches to a few feet thick, intermixed with zones containing disseminated sulfides and barren zones (Frank Canney, oral communica-

tuting a pair of orthogonal electric field dipoles at one of the stations for the two vertical sensors; this substitution is necessary because only 6 data acquisition channels are available. The horizontal fields measured at the second station are used as the reference.

The 6 digital time series are each 64 points long. They are displayed graphically for visual inspection, allowing rejection of time series that exceeded the dynamic range, which are particularly noisy, or which have very low amplitude. The Fourier spectra of the acceptable time series are transferred from the digital signal processor to the computer. The computer forms the cross-spectral matrix from the 6 spectra and averages the cross-spectra both in time and frequency. The first 20 Fourier harmonics are averaged into 4 frequency bands spanning slightly more than 2½ octaves in frequency. The average cross spectra of 8 sets of time series are stored as a single block on the digital cassette tape allowing for additional processing at a later date. The tipper or impedance results are computed from the subsequent average of these data blocks. Adequate results were generally obtained from two blocks, representing 16 sets of time series, for the tipper or from three blocks, 24 sets of time series, for the impedance. The data are acquired in several overlapping frequency bands. Each station required approximately 45 to 60 minutes to complete.

The entire system weighs approximately 120 lb and can be carried by a crew of three. The 6 magnetic field sensors at over 40 lb, and the analog filters and digital signal processor, which are mounted on a backpack frame, at 45 lb account for most of the weight. The computer, wire, electrodes, oscilloscope, and batteries form the rest. The filters and digital signal processor are powered by a 12 V lead-acid motorcycle
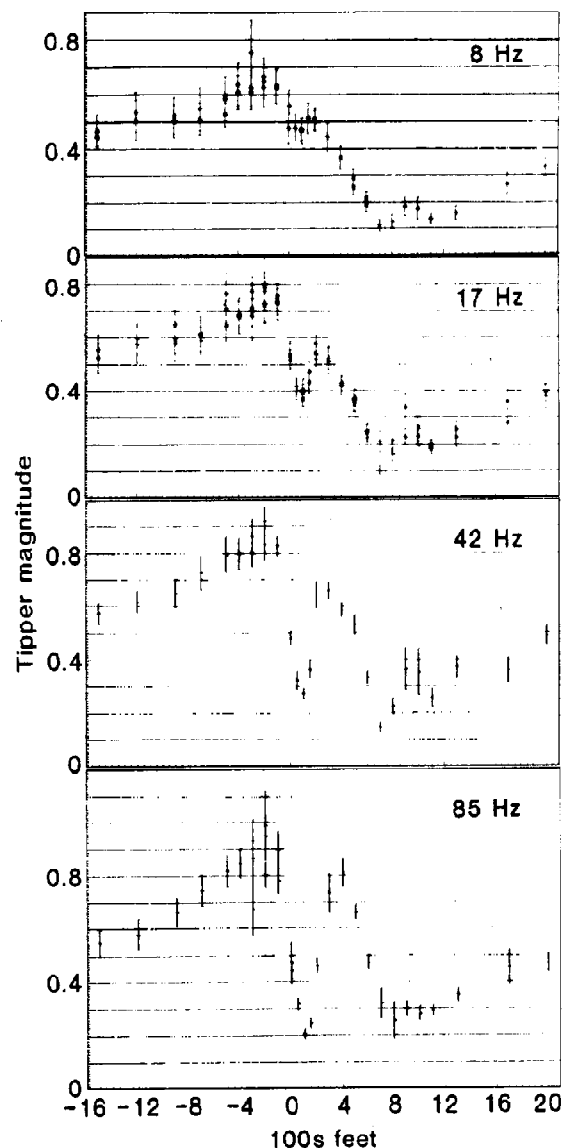

FIG. 3. Line 54W tipper magnitude at 8, 17, 42, and 85 Hz.

tion, 1983). Pyrrhotite is the dominant sulfide mineral but there are sub-ore grade amounts of pentlandite and chalcopyrite.

The presence of the mineralization was first indicated by a geochemical stream sediment and soil survey and an Input electromagnetic anomaly. The deposit is under 1-15 ft of glacial till and was outlined by a slingram survey prior to drilling. Slingram results and the interpreted conductors for the southwestern half of the mineralized zone are indicated in Figure 2; the total length of the main conductor is about 2 300 ft and its width, as sensed by slingram, varies from about 20 to 200 ft. There are no slingram anomalies northwest of the deposit and VLF measurements indicate that the host rock resistivities are on the order of several thousand

ohm-m. There are a number of slingram anomalies and low VLF resistivity anomalies on the south side of the mineralized zone that are caused by pyrrhotitic slates. From the VLF measurements, or from slingram measurements made with a large coil separation (400 ft), it is difficult to distin-
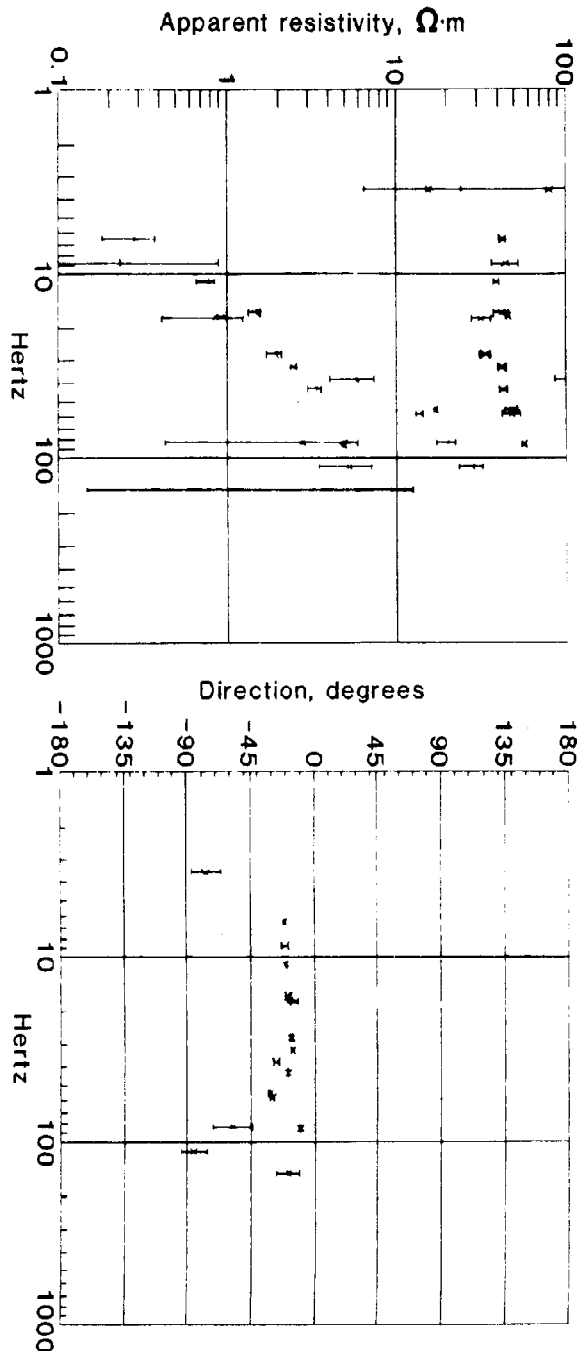

Fig. 4. Apparent resistivity and principal direction; station 54W-200N.
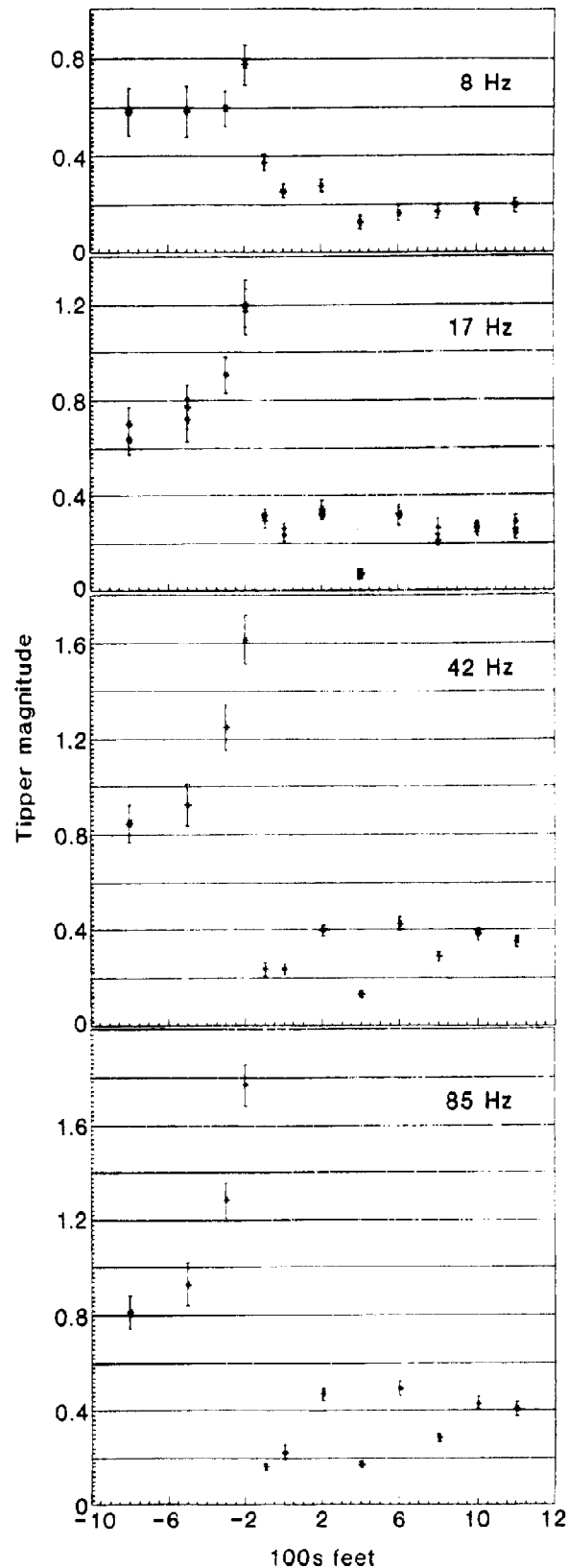

Fig. 5. Line 48W tipper magnitude at 8, 17, 42, and 85 Hz.

guish between the anomalies caused by the sulfide hornfels and those caused by the deposit because both conductors yield a saturation response. However, by using a 100 ft coil separation and a low frequency, one can readily distinguish the two types of conductors with slingram measurements. The resistivity of the upper part of the deposit was estimated from slingram results to be on the order of 0.01 Ω-m.

Field test results

Two tipper profiles were run along lines 54W and 48W during the last week of September and the first week of October 1983. At this time the natural field's spectral amplitudes in the 1–100 Hz frequency band were high relative to the internal noise levels of the magnetic field sensors. Tipper results on line 54W appear to be reasonably two-dimensional (Figure 3). This may be fortuitous as the profile is within about 300 ft of the end of the principal conductor as mapped by slingram. The conductor may continue along strike at depth. The responses of two conductors are clear at the higher frequencies. The more conductive deposit has a larger response and peaks at a lower frequency than the southern hornfels conductor. This is consistent with the slingram interpretation. Reasonable impedance estimates were obtained even though the electric field measurements proved to be noisier than expected. An example of the apparent resistivity and principal direction (Figure 4) is shown for station 54W-200N, a site very near the contact.

Tipper data for line 48W (Figure 5) show a distinct 3-D response at higher frequencies. The tipper amplitude is much larger than can be explained by a 2-D model. Examination of the slingram profiles shows that the principal conductor body narrows considerably in the vicinity of line 48W. It seems reasonable to assume that local currents induced in the wide parts of the conductor are channeled through the narrow part giving rise to a larger vertical magnetic field than can be predicted for a two dimensional body.

Discussion

The field test demonstrates that remote referenced tensor tipper and MT impedance data can be acquired and processed in the field with a portable system. A reduction in weight so that a crew of two could transport the system could be easily accomplished by repackaging the instruments and redesigning the sensors. The receiver's high frequency limit could be raised by the implementation of improved analog filters. Lower frequencies could be used by simply changing sensors. It is expected that with these improvements, systems capable of making portable tipper and magnetotelluric measurements will be useful geophysical tools.

References

Espenshade, G. H., 1972, Geology of the Moxie pluton in the Moosehead Lake-Jo-Mary Mountain Area, Piscataquis County, Maine: U.S.G.S. Bull. 1340, 40 p.

Gamble, T. D., Gouban, W. M., and Clarke, J., 1979, Magnetotellurics with a remote reference: Geophysics, 44, 53–68.

Jupp, D. L., and Vozoff, K., 1976, On: The magnetotelluric method in the exploration of sedimentary basins: Geophysics, 41, 325–328.

Morrison, H. F., Goldstein, N. E., Hoversten, M., Oppliger, G., and Riveros, C., 1978, Description, field test, and data analysis of a controlled-source EM system (EM-60): Univ. of California–Lawrence Berkeley Lab Tech. rep. LBL7088, 150 p.

Applications of CSAMT in Mapping Structure and Alteration Associated with Petroleum   EM4.4

L. J. Hughes, N. R. Carlson, and A. G. Ostrander, Zonge Engineering & Research Organization, Inc.

Examples of two distinct applications of the controlled source audio-frequency magnetotellurics (CSAMT) technique to petroleum exploration are provided by data collected over fields in Nevada and Oklahoma. At Trap Spring field, a structural fault-truncation trap in the Basin and Range province, CSAMT data provide an accurate map of lithology, the valley fill/basement contact, and major basin-margin fault structure related to the trap. The electrical interpretation is substantiated by air photo, seismic, and geologic data for the area. A second example involves the mapping of electrochemical alteration overlying the stratigraphic gas trap at Ashland field, located in Oklahoma's Arkoma basin. A resistive surface layer and a deeper conductive plume were detected over the field by CSAMT data. These appear to be causally linked to upward migration of hydrocarbons from the trap and subsequent mineralization and cementation processes, documented earlier by Oehler and Sternberg (1982).

These two field examples and the inherent capabilities of CSAMT suggest a wider role for this technique in multidisciplinary exploration and development for both structurally and stratigraphically trapped hydrocarbons.

Introduction

The controlled source audio-frequency magnetotelluric (CSAMT) method has been described previously in the literature (Goldstein and Strangway, 1975; Sandberg and Hohmann, 1982). CSAMT is a vertical sounding technique similar in many respects to the more widely used magnetotellurics (MT) technique, with the exception that it utilizes a dipole or loop as a fixed signal source instead of naturally occurring earth tellurics. This results in a more dependable signal source and significantly reduces the complexity and cost of the necessary field instrumentation. CSAMT measurements are usually made in the far-field or plane-wave regime some 5 to 10 km away from the source. The normal application, and the one used in this paper, is to measure the horizontal electric field magnitude and phase angle across a dipole oriented parallel to the source dipole, and the horizontal magnetic field magnitude and phase angle from an antenna oriented perpendicular to the source dipole. The ratio of the electric and magnetic field magnitudes then yields the Cagniard apparent resistivity. The difference between the electric and magnetic field phase angles yields the phase difference, which is conceptually related to the derivative of the resistivities. Measurements are made at a suite of frequencies in the 1 to 4 096 Hz range in order to construct an electrical pseudosection.

CSAMT has been used for massive sulfide detection (Zonge et al., 1980), geothermal work (Sandberg and Hohmann, 1982), for monitoring enhanced oil recovery processes and coal gasification (Bartel and Wayland, 1981; Bartel, 1982), and in other applications ranging from engineering geophysics to precious metal exploration. Recently, CSAMT was applied to petroleum exploration (Ostrander et al., 1983) due to its decreased sensitivity to culture, lower cost, and directness of interpretation with respect to complex resistiv-